Received: *August 17, 1998*, Accepted: *October 14, 1998*

Tagged photons in DIS with next-to-leading accuracy

Harald Anlauf*

Fachbereich Physik, Siegen University, 57068 Siegen, Germany
E-mail: anlauf@hep.tu-darmstadt.de

Andrej B. Arbuzov, Eduard A. Kuraev

Bogoliubov Laboratory of Theoretical Physics, JINR, Dubna, 141980, Russia
E-mail: arbuzov@thsun1.jinr.ru, kuraev@thsun1.jinr.ru

Nicolai P. Merenkov

Institute of Physics and Technology, Kharkov, 310108, Ukraine
E-mail: merenkov@kipt.kharkov.ua

Abstract: The leading and next-to-leading radiative corrections to deep inelastic events with tagged photons are calculated analytically. Comparisons with previous results and numerical estimations are presented for the experimental conditions at HERA.

Keywords: Standard Model, Electromagnetic Processes and Properties.

*Supported by Bundesministerium für Bildung, Wissenschaft, Forschung und Technologie (BMBF), Germany.

Contents

1. Introduction

It is well known that the radiative corrections to deep inelastic electron proton scattering due to hard real photon emission are very important in certain regions of the HERA kinematic domain. In fact, the initial-state collinear radiation leads to a reduction of the projectile electron energy and therefore to a shift of the effective Bjorken variables in the hard scattering process as compared to those determined from the actual measurement of the scattered electron alone. Therefore, radiative events

$$e(p_1) + p(P) \to e(p_2) + \gamma(k) + X + (\gamma) \tag{1.1}$$

are to be carefully taken into account [1, 2, 3].

On the other hand, measuring the energy of the photons emitted very close to the incident electron beam direction [4, 5, 6, 7] permits to overlap the kinematical region of photoproduction ($Q^2 \approx 0$) and the DIS region with small transferred momenta (about a few GeV^2) within the high energy HERA experiments. Furthermore, these radiative events may be used to independently determine the proton structure functions F_2 and F_1 (and therefore F_L) in a single run without lowering the beam energies [5, 8]. Preliminary results of an F_2 analysis using such radiative events were recently presented by the H1 collaboration [9].

Our aim is to calculate the radiative corrections to neutral current deep inelastic events with simultaneous (exclusive) detection of a hard photon emitted very close to the direction of the incoming electron beam ($\theta_\gamma = \widehat{\boldsymbol{p}_1\boldsymbol{k}} \le \theta_0 \approx 5 \cdot 10^{-4}$ rad). In the case of the HERA collider, the experimental detection of photons emitted in this very forward direction is actually possible due to the presence of photon detectors (PD) that are part of the luminosity monitoring system of ZEUS and H1.

Let us briefly review the kinematics for the process under consideration. As the opening angle of the forward photon detector is very small, and since we will only consider cross sections where the tagged photon is integrated over the solid angle covered by this photon detector, we can parameterize these radiative events using the standard Bjorken variables x and y, that are determined from the measurement of the scattered electron,

$$x = \frac{Q^2}{2P\cdot(p_1-p_2)}\,, \quad y = \frac{2P\cdot(p_1-p_2)}{V}\,,$$
$$Q^2 = 2p_1\cdot p_2 = xyV, \quad \text{with} \quad V = 2P\cdot p_1\,, \tag{1.2}$$

and the energy fraction z of the electron after initial state radiation of a collinear photon,

$$z = \frac{2P\cdot(p_1-k)}{V} = \frac{\varepsilon-k^0}{\varepsilon}\,, \tag{1.3}$$

where ε is the initial electron energy, and k^0 is the energy seen in the forward photon detector.

An alternative set of kinematic variables that is especially adapted to the case of collinear radiation, is given by the *shifted* Bjorken variables [5]

$$\hat{Q}^2 = -(p_1-p_2-k)^2\,, \qquad \hat{x} = \frac{\hat{Q}^2}{2P\cdot(p_1-p_2-k)}\,, \qquad \hat{y} = \frac{P\cdot(p_1-p_2-k)}{P\cdot(p_1-k)}\,. \tag{1.4}$$

The relations between the shifted and the standard Bjorken variables read [5]

$$\hat{Q}^2 = zQ^2\,, \qquad \hat{x} = \frac{xyz}{z+y-1}\,, \qquad \hat{y} = \frac{z+y-1}{z}\,. \tag{1.5}$$

The cross-section under consideration in the Born approximation, integrated over the solid angle of the photon detector ($0 \le \theta_\gamma \le \theta_0,\ \theta_0 \ll 1$) then takes the following form:

$$\frac{z}{y}\frac{\mathrm{d}^3\sigma_{\mathrm{Born}}}{\mathrm{d}x\,\mathrm{d}y\,\mathrm{d}z} = \frac{1}{\hat{y}}\frac{\mathrm{d}^3\sigma_{\mathrm{Born}}}{\mathrm{d}\hat{x}\,\mathrm{d}\hat{y}\,\mathrm{d}z} = \frac{\alpha}{2\pi}P(z,L_0)\tilde{\Sigma}\,, \tag{1.6}$$

where

$$\tilde{\Sigma} = \Sigma(\hat{x},\hat{y},\hat{Q}^2) = \frac{2\pi\alpha^2(-\hat{Q}^2)}{\hat{Q}^2\hat{x}\hat{y}^2}F_2(\hat{x},\hat{Q}^2)\left[2(1-\hat{y}) - 2\hat{x}^2\hat{y}^2\frac{M^2}{\hat{Q}^2} + \left(1+4\hat{x}^2\frac{M^2}{\hat{Q}^2}\right)\frac{\hat{y}^2}{1+R}\right],$$

$$P(z,L_0) = \frac{1+z^2}{1-z}L_0 - \frac{2z}{1-z}\,, \quad R = R(\hat{x},\hat{Q}^2) = \left(1+4\hat{x}^2\frac{M^2}{\hat{Q}^2}\right)\frac{F_2(\hat{x},\hat{Q}^2)}{2\hat{x}F_1(\hat{x},\hat{Q}^2)}\,, -1\,,$$

$$\alpha(-\hat{Q}^2) = \frac{\alpha}{1-\Pi(-\hat{Q}^2)}\,, \quad L_0 = \ln\left(\frac{\varepsilon^2\theta_0^2}{m^2}\right)\,, \quad \hat{Q}^2 = 2zp_1\cdot p_2 = 2z\varepsilon^2Y(1-c)\,,$$

$$Y = \frac{\varepsilon_2}{\varepsilon} = 1 - y + xy\frac{E_p(1+\beta_p)}{2\varepsilon}\,, \quad c = \cos(\widehat{\boldsymbol{p}_1\boldsymbol{p}_2})\,,$$
$$\hat{x} = \frac{\hat{Q}^2}{2P\cdot(zp_1-p_2)} = \frac{z\varepsilon Y(1-c)}{zE_p(1+\beta_p) - YE_p(1+\beta_p c)}\,, \quad \beta_p = \sqrt{1-M^2/E_p^2}\,,$$
$$\hat{y} = \frac{2P\cdot(zp_1-p_2)}{zV} = \frac{z(1+\beta_p)-Y(1+\beta_p c)}{z(1+\beta_p)}\,. \tag{1.7}$$

The quantities F_2 and F_1 are the proton structure functions; M and m are the proton and electron masses, respectively. In the cross-section (1.6) we take into account terms proportional to $M^2/\hat{Q}^2$, which may be important at low Q^2. Note that the neglect of Z-boson exchange and γ–Z interference is a good approximation, because we are interested mostly in events with small momentum transfer $\hat{Q}^2$.[1] The energies of the initial and final electron, of the tagged photon and of the initial proton (ε, ε_2, k^0 and E_p) are defined in the laboratory reference frame (i.e., the rest frame of HERA detectors). The cross section (1.6) agrees with [5, 6]. Also note that we explicitly included the correction from the vacuum polarization operator $\Pi(-\hat{Q}^2)$ in the virtual photon propagator. The aim of our work is to calculate the higher order QED radiative corrections for this process in the leading and next-to-leading logarithmic approximation.

In this paper we restrict ourselves to the model independent QED radiative corrections related to the lepton line, which form a complete, gauge invariant subset for the neutral current scattering process. The remaining source of QED radiative corrections at the same order, such as virtual corrections with double photon exchange and bremsstrahlung off the partons are more involved and model dependent, they will be considered elsewhere. Our approach to the calculation of the QED corrections is based on the utilization of all essential Feynman diagrams that describe the observed cross-section in the framework of the used approximation. The same approach was used recently for the calculation of the QED corrections for the small angle Bhabha scattering cross-section at LEP1 [10]. This work extends our previous calculation at the leading logarithmic level [11] and presents the details of the brief outline published in [12].

The paper is organized as follows. Section 2 is devoted to the corrections related with emission of virtual and soft real photons in the hard collinear photon emission DIS process. In sect. 3 we consider the radiative corrections due to emission of two hard photons in the collinear kinematics (where we distinguish between the cases when both photons are emitted close to the initial electron direction and the case when one of the photons is emitted along the initial and the other one along the scattered electron direction) and the semi-collinear kinematics, where the additional hard photon is emitted at a large angle. Section 4 collects the results obtained and discusses two experimental cases: an exclusive set-up, that assumes that a bare electron can be measured, and a calorimetric one. We show that, in the latter case for a coarse detector that performs

[1]The corresponding Born cross section including contributions from the Z can be found in ref. [6].

a calorimetric measurement, we can reproduce the result of our previous paper [11], where the leading logarithmic approximation was used and where the emission along the final electron was not taken into account. In conclusion we give some numerical estimates. The appendices are devoted to details of the calculation.

2. Virtual and soft corrections

In order to calculate the contributions from the virtual and soft photon emission corrections, we start from the expression for the Compton scattering tensor with a heavy photon [13],

$$K_{\mu\nu} = (8\pi\alpha)^{-1} \sum_{\text{spins}} M_\mu^{e\gamma^* \to e'\gamma} (M_\nu^{e\gamma^* \to e'\gamma})^* \,, \tag{2.1}$$

where M_μ is the matrix element of the process of Compton scattering

$$\gamma^*(-q) + e(p_1) \to \gamma(k) + e(p_2) \,, \tag{2.2}$$

and the index μ describes the polarization state of the virtual photon. This tensor is conveniently decomposed as follows:

$$\begin{aligned} K_{\mu\nu} &= \frac{1}{2}(P_{\mu\nu} + P^*_{\nu\mu}) \,, \qquad (2.3)\\ P_{\mu\nu} &= \tilde{g}_{\mu\nu}(B_g + \frac{\alpha}{2\pi}T_g) + \tilde{p}_{1\mu}\tilde{p}_{1\nu}(B_{11} + \frac{\alpha}{2\pi}T_{11}) + \\ &\quad + \tilde{p}_{2\mu}\tilde{p}_{2\nu}(B_{22} + \frac{\alpha}{2\pi}T_{22}) + \frac{\alpha}{2\pi}(\tilde{p}_{1\mu}\tilde{p}_{2\nu}T_{12} + \tilde{p}_{2\mu}\tilde{p}_{1\nu}T_{21}), \\ \tilde{g}_{\mu\nu} &= g_{\mu\nu} - \frac{q_\mu q_\nu}{q^2}\,, \quad \tilde{p}_{1\mu} = p_{1\mu} - q_\mu\frac{p_1 \cdot q}{q^2}\,, \quad \tilde{p}_{2\mu} = p_{2\mu} - q_\mu\frac{p_2 \cdot q}{q^2}\,, \quad p_1 = q + p_2 + k\,. \end{aligned}$$

The expressions for the quantities B_{ij} corresponding to the Born approximation are:[2]

$$\begin{aligned} B_g &= \frac{1}{st}\left[(s+u)^2 + (t+u)^2\right] - 2m^2q^2\left(\frac{1}{s^2} + \frac{1}{t^2}\right), \qquad B_{11} = \frac{4q^2}{st} - \frac{8m^2}{s^2}\,, \\ B_{22} &= \frac{4q^2}{st} - \frac{8m^2}{t^2}\,, \qquad s = 2p_2 \cdot k\,, \quad t = -2p_1 \cdot k, \quad u = (p_2 - p_1)^2\,, \\ q^2 &= s + t + u, \quad p_1^2 = p_2^2 = m^2, \quad k^2 = 0\,. \end{aligned} \tag{2.4}$$

The one-loop QED corrections are contained in the quantities T_{ij}, whose explicit expressions are given in [13]. Here we have to integrate them over the solid angle of the emitted photon corresponding to the shape of the photon detector. We need to keep only the terms singular in the limit $\theta_\gamma \to 0$, since after integration the constant terms contribute only proportional to $\theta_0^2 \sim 10^{-6}$ and can be safely neglected. Another

[2]We have already dropped those terms that vanish in the high-energy limit when one integrates over any finite region of photon phase space.

simplification comes from the fact that we need only the symmetric (and real) part of the tensor K. This way, by using typical integrals

$$\int \frac{\mathrm{d}\Omega_k}{2\pi}\frac{1}{t} = -\frac{L_0}{2\varepsilon^2(1-z)}\,, \qquad \int \frac{\mathrm{d}\Omega_k}{2\pi}\frac{m^2}{t^2} = \frac{1}{2\varepsilon^2(1-z)^2}\,, \tag{2.5}$$

and using the expressions given in Appendix A we obtain the following expression for the Compton tensor integrated over the angular part of the photon phase space:

$$\int \frac{\mathrm{d}\Omega_k}{2\pi}K_{\mu\nu} = \left(-Q_l^2 g_{\mu\nu} + 4zp_{1\mu}p_{1\nu}\right)\frac{1}{2\varepsilon^2(1-z)}\left[\left(1+\frac{\alpha}{2\pi}\rho\right)P(z,L_0) - \frac{\alpha}{2\pi}T\right], \tag{2.6}$$

$$\begin{aligned}
\rho &= 4\ln\frac{\lambda}{m}(L_Q-1) - L_Q^2 + 3L_Q + 3\ln z + \frac{\pi^2}{3} - \frac{9}{2}\,,\\
T &= \frac{1+z^2}{1-z}(A\ln z + B) - \frac{4z}{1-z}L_Q\ln z - \frac{2-(1-z)^2}{2(1-z)}L_0 + \mathcal{O}(\mathrm{const})\,,\\
A &= -L_0^2 + 2L_0L_Q - 2L_0\ln(1-z), \quad B = \left(\ln^2 z - 2\mathrm{Li}_2(1-z)\right)L_0\,,\\
L_Q &= \ln\frac{Q^2}{m^2}\,, \qquad \mathrm{Li}_2(x) = -\int\limits_0^x \frac{\mathrm{d}y}{y}\ln(1-y)\,.
\end{aligned}$$

The quantity λ, which enters into the expression for ρ, is a fictitious photon mass.

In the construction of the total expression for the tensor $K_{\mu\nu}$ we replaced $q_\mu = q_\nu = 0$, $p_{2\mu,\nu} = zp_{1\mu,\nu}$, bearing in mind the gauge invariance of hadronic tensor [14],

$$\begin{aligned}
H_{\mu\nu} &= \frac{4\pi}{M}\left(W_2(x_h,Q_h^2)\tilde{P}_\mu\tilde{P}_\nu - M^2W_1(x_h,Q_h^2)\tilde{g}_{\mu\nu}\right), \quad x_h = \frac{Q_h^2}{2P\cdot q_h}\,, \\
\tilde{P}_\nu &= P_\nu - q_{h\nu}\frac{P\cdot q_h}{q_h^2}\,.
\end{aligned} \tag{2.7}$$

Here we imply $q_h = q$, $Q_h^2 = -q^2$.

Consider now the process with emission of a soft photon in addition to the emission of the hard one, which hits the PD. We imply the condidtion that the energy of the soft photon should be less than some small quantity $\delta\varepsilon$ (in the center–of–mass system). In straightforward calculations, starting from Feynman diagrams, some care is to be paid in the evaluation of integrals over the phase volume of the soft photon, as some contributions are crucially dependent on the correlation between our two small parameters $\Delta = \delta\varepsilon/\varepsilon$ and θ_0. In our particular case $\theta_0 \ll \Delta \ll 1$, the result coincides with the one obtained using the approximation of classical currents for soft photons. The total effect for the sum of contributions of virtual and soft photon emission consists in the replacement of the quantity ρ by $\tilde{\rho}$ in eq. (2.6) (see eq. (45) in [13]):

$$\rho \to \tilde{\rho} = 2(L_Q-1)\ln\frac{\Delta^2}{Y} + 3L_Q + 3\ln z - \ln^2 Y - \frac{\pi^2}{3} - \frac{9}{2} + 2\mathrm{Li}_2\left(\frac{1+c}{2}\right). \tag{2.8}$$

The final expression for the virtual and soft photon emission corrected tagged photon cross-section has the form

$$\frac{z}{y}\frac{\mathrm{d}^3\sigma_{VS}}{\mathrm{d}x\,\mathrm{d}y\,\mathrm{d}z} = \left(\frac{\alpha}{2\pi}\right)^2\left[P(z,L_0)\tilde{\rho} - T\right]\tilde{\Sigma}\,. \tag{2.9}$$

3. Double hard bremsstrahlung

Consider now the emission of an extra photon with the energy more than $\delta\varepsilon$. For the calculation of the contributions from real hard bremsstrahlung, which in our case correspond to double photon emission with at least one photon seen in the forward detector, we specify three specific kinematical domains: *i)* both hard photons strike the forward photon detector, i.e., both are emitted within a narrow cone around the electron beam ($\theta \leq \theta_0$); *ii)* one hard photon is tagged by the PD, while the other is collinear to the outgoing electron ($\theta_2 = \widehat{\boldsymbol{k}_2\boldsymbol{p}_2} \leq \theta_0'$); and finally *iii)* the second photon is emitted at large angles (i.e., outside the defined narrow cones) with respect to both incoming and outgoing electron momenta. We denominate the third kinematical domain as a semi-collinear one. The contributions of the regions *i)* and *ii)* contain leading terms (quadratic in the large logarithms L_0, L_Q), whereas region *iii)* contains formally non-leading terms of order $L_0\ln(1/\theta_0^2)$, which, however, give a contribution numerically larger than the leading ones since $\varepsilon\theta_0/m \ll 1/\theta_0$.

The calculation beyond the leading logarithmic approximation may be performed using the results of a paper of one of us [16]. The contribution from the kinematical region *i)* (both hard photons being tagged), has the form (see eq. (Π 6) from [16]):

$$\frac{z}{y}\frac{\mathrm{d}^3\sigma_i^{\gamma\gamma}}{\mathrm{d}x\,\mathrm{d}y\,\mathrm{d}z} = \frac{\alpha^2}{8\pi^2}L_0\biggl[L_0\biggl(P_\Theta^{(2)}(z) + 2\frac{1+z^2}{1-z}\Bigl(\ln z - \frac{3}{2} - 2\ln\Delta\Bigr)\biggr) + 6(1-z) + \\ + \Bigl(\frac{4}{1-z} - 1 - z\Bigr)\ln^2 z - 4\frac{(1+z)^2}{1-z}\ln\frac{1-z}{\Delta}\biggr]\tilde{\Sigma} + \\ + \mathcal{O}(\mathrm{const})\,. \qquad (3.1)$$

Here we use the notation $P_\Theta^{(2)}(z)$ for the Θ-part of the second order term of the expansion of the electron non-singlet structure function

$$\begin{aligned} D(z,L) &= \delta(1-z) + \frac{\alpha}{2\pi}P^{(1)}(z)L + \frac{1}{2}\Bigl(\frac{\alpha}{2\pi}\Bigr)^2 P^{(2)}(z)L^2 + \dots\,, \\ P^{(i)}(z) &= P_\Theta^{(i)}(z)\Theta(1-z-\Delta) + P_\delta^{(i)}\delta(1-z), \quad \Delta \to 0\,, \\ P_\Theta^{(1)}(z) &= \frac{1+z^2}{1-z}, \quad P_\delta^{(1)} = \frac{3}{2} + 2\ln\Delta\,, \\ P_\Theta^{(2)}(z) &= 2\biggl[\frac{1+z^2}{1-z}\Bigl(2\ln(1-z) - \ln z + \frac{3}{2}\Bigr) + \frac{1}{2}(1+z)\ln z - 1 + z\biggr]. \end{aligned} \qquad (3.2)$$

The parameter Δ serves as the infrared regularization parameter.

The contribution of the kinematical region *ii)* to the observed cross-section depends on the event selection; in other words, on the method of measurement of the scattered particles.

In the case of exclusive event selection, when only the scattered electron is detected, while the photon that is emitted almost collinearly (i.e., within a small cone with opening angle $2\theta_0'$ around the momentum of the outgoing electron) goes unnoticed or is not taken into account in the determination of the kinematical variables, we have (see П8 from [16])

$$\frac{z}{y}\frac{\mathrm{d}^3\sigma_{ii}^{\gamma\gamma}}{\mathrm{d}x\,\mathrm{d}y\,\mathrm{d}z} = \frac{\alpha^2}{4\pi^2}P(z,L_0)\int\limits_{\Delta/Y}^{y_2^{\max}}\frac{\mathrm{d}y_2}{1+y_2}\left[\frac{1+(1+y_2)^2}{y_2}(\tilde{L}-1)+y_2\right]\Sigma_s\,,$$
$$\Sigma_s = \Sigma(x_b,y_b,Q_b^2)\,, \tag{3.3}$$

where

$$\tilde{L} = \ln(\varepsilon\theta_0'/m)^2 + 2\ln Y, \quad y_2 = \frac{x_2}{Y}, \quad Y = \varepsilon_2/\varepsilon, \quad y_2^{\max} = \frac{2z - Y(1+c)}{Y(1+c)}\,,$$
$$x_b = \frac{xyz(1+y_2)}{z-(1-y)(1+y_2)}, \quad y_b = \frac{z-(1-y)(1+y_2)}{z}, \quad Q_b^2 = Q^2 z(1+y_2)\,. \tag{3.4}$$

More realistic (from the experimental point of view) is the calorimetric event selection, when only the sum of the energies of the outgoing electron and photon can be measured if the photon momentum lies inside the small cone with opening angle $2\theta_0'$ along the direction of the final electron. In this case we find

$$\frac{z}{y}\frac{\mathrm{d}^3\sigma_{ii,cal}^{\gamma\gamma}}{\mathrm{d}x\,\mathrm{d}y\,\mathrm{d}z} = \frac{\alpha^2}{4\pi^2}P(z,L_0)\int\limits_{\Delta/Y}^{\infty}\frac{\mathrm{d}y_2}{(1+y_2)^3}\left[\frac{1+(1+y_2)^2}{y_2}(\tilde{L}-1)+y_2\right]\tilde{\Sigma}$$
$$= \frac{\alpha^2}{4\pi^2}P(z,L_0)\left[(\tilde{L}-1)\left(2\ln\frac{Y}{\Delta}-\frac{3}{2}\right)+\frac{1}{2}\right]\tilde{\Sigma}\,. \tag{3.5}$$

In the last equation we used the relation

$$\Sigma_s = \frac{1}{(1+y_2)^2}\tilde{\Sigma}\,, \tag{3.6}$$

which is valid for the calorimetric set-up.

Consider at last the semi-collinear region *iii)*. The relevant contribution may be calculated using the quasireal electron method [15]:

$$\frac{z}{y}\frac{\mathrm{d}^3\sigma_{iii}^{\gamma\gamma}}{\mathrm{d}x\,\mathrm{d}y\,\mathrm{d}z} = \frac{\alpha}{2\pi}P(z,L_0)\frac{2\alpha}{\pi}\int\frac{\mathrm{d}^3k_2}{\omega_2}\frac{\alpha^2(Q_{sc}^2)}{Q_{sc}^4}I^\gamma\,, \tag{3.7}$$
$$I^\gamma = B_{\rho\sigma}(zp_1,p_2,k_1)H^{\rho\sigma}/(8\pi)\,.$$

The quantity $B_{\rho\sigma}(zp_1,p_2,k_1)$ is obtained from equation (2.4), where it necessary to set $m=0$. After some algebraic transformations we obtain

$$I^\gamma = \frac{1}{st}\Bigg[F_2(x_{sc},Q_{sc}^2)\Bigg(\frac{M^2}{Q_{sc}^2}x_{sc}G - V\Big[x_{sc}(z^2+(1-y)^2)V + (1-y)(zQ^2-s) -$$
$$- z(zQ^2-t)\Big]\Bigg) - GF_1(x_{sc},Q_{sc}^2)\Bigg], \qquad G = z^2Q^4 - 2st + Q_{sc}^4\,, \tag{3.8}$$
$$x_{sc} = \frac{Q_{sc}^2}{V(z+y-1)-2P\cdot k_2}, \quad s = 2p_2\cdot k_2\,, \quad t = -2zp_1\cdot k_2\,, \quad Q_{sc}^2 = zQ^2 - s - t\,.$$

The angular integration in eq. (3.7) is to be performed over the whole phase space, excepting the small cones along directions of motion of the initial and scattered electrons that correspond to the kinematic regions *i)* or *ii)*. The result (for the details see Appendix B) has the form

$$\frac{z}{y}\frac{\mathrm{d}^3\sigma_{iii}^{\gamma\gamma}}{\mathrm{d}x\,\mathrm{d}y\,\mathrm{d}z} = \left(\frac{\alpha}{2\pi}\right)^2 P(z,L_0)\Bigg[\int\limits_{\Delta}^{x_2^t}\frac{\mathrm{d}x_2}{x_2}\frac{z^2+(z-x_2)^2}{z(z-x_2)}\ln\frac{2(1-c)}{\theta_0^2}\Sigma_t + \\ + \int\limits_{\Delta}^{x_2^s}\frac{\mathrm{d}x_2}{x_2}\frac{1+(1+y_2)^2}{1+y_2}\ln\frac{2(1-c)}{\theta_0'^2}\Sigma_s + Z\Bigg], \tag{3.9}$$

$$\Sigma_t = \Sigma(x_t, y_t, Q_t^2)\,, \tag{3.10}$$

The logarithmic dependencies on the infrared regulator Δ and on the angles θ_0, θ_0' are fully contained in the first two terms on the r.h.s., whereas the quantity Z represents an integral over the whole photon phase space of a well-behaved function, and it is free from collinear and infrared singularities. Its explicit expression is given in Appendix B.

The upper limits of the x_2-integration in (3.9) read

$$x_2^t = z - \frac{Y(1+c)}{2}\,, \qquad x_2^s = \frac{2z - Y(1+c)}{1+c}\,, \tag{3.11}$$

and the arguments of Σ_t are

$$x_t = \frac{xy(z-x_2)}{z-x_2+y-1}\,, \quad y_t = \frac{z-x_2+y-1}{z-x_2}, \quad Q_t = Q^2(z-x_2). \tag{3.12}$$

An explicit expression for x_m, which is relevant for the calculation of Z, is given in Appendix B.

The formulae given above (see eqs. (1.7), (2.9), (3.1), (3.3) or (3.5), and (3.9)) provide the complete answer for the leading and subleading contributions up to the second order of perturbation theory. The total sum of virtual, soft, and hard additional photons emission corrections to the radiative DIS cross section does not depend on the auxiliary parameter $\Delta = \delta\varepsilon/\varepsilon$, as it should be.

4. Results for different experimental situations

The sum of the contributions of the leading and next-to-leading corrections at order α^2, which are given explicitly in expressions (2.9), (3.1), (3.3) or (3.5), and (3.9), may be written in the form

$$\frac{z}{y}\frac{\mathrm{d}^3\sigma}{\mathrm{d}x\,\mathrm{d}y\,\mathrm{d}z} = \left(\frac{\alpha}{2\pi}\right)^2(\Sigma_i + \Sigma_f)\,. \tag{4.1}$$

JHEP10(1998)013

The first term Σ_i is independent of the experimental selection of the scattered electron and has the form

$$\Sigma_i = \left\{ \frac{1}{2} L_0^2 P_\Theta^{(2)}(z) + P(z, L_0) \left[\frac{1 - 16z - z^2}{2(1+z^2)} + \left(3 - 2\ln Y + \frac{4z}{1+z^2} \right) \ln z + \right.\right.$$
$$\left.\left. + \ln^2 Y - 2\mathrm{Li}_2(z) + 2\mathrm{Li}_2\left(\frac{1+c}{2}\right) - \frac{2(1+z)^2}{1+z^2} \ln(1-z) + \frac{1-z^2}{2(1+z^2)} \ln^2 z \right]\right\} \tilde{\Sigma} +$$
$$+ P(z, L_0)\, \tilde{\Sigma} \ln \frac{2(1-c)}{\theta_0^2} \left[\int\limits_0^{u_0} \frac{\mathrm{d}u}{u} (1 + (1-u)^2) \left(\frac{\Sigma_t}{(1-u)\tilde{\Sigma}} - 1 \right) - \right. \tag{4.2}$$
$$\left. - \int\limits_{u_0}^{1} \frac{\mathrm{d}u}{u} (1 + (1-u)^2) \right] + P(z, L_0)\, Z, \qquad u = \frac{x_2}{z}\,, \quad u_0 = \frac{x_2^t}{z}\,,$$

where Z is given in Appendix B and the remaining notations are as above (see (3.1), (3.8), and (3.11)).

The second term in (4.1), denoted Σ_f, however, does explicitly depend on the event selection. It corresponds to the emission of a hard photon by the scattered electron. In the exclusive set-up, when only the scattered bare electron is measured, while the photon that is emitted close to the final electron's direction is ignored, this contribution reads

$$\Sigma_f = \Sigma_f^{excl} = P(z, L_0) \int\limits_0^{x_2^s/Y} \mathrm{d}y_2 \left[\left(\frac{1 + (1+y_2)^2}{y_2} (L_Q + \ln Y - 1) + y_2 \right) \frac{1}{1+y_2} \times \right.$$
$$\left. \times \Theta\left(y_2 - \frac{\Delta}{Y} \right) + (L_Q + \ln Y - 1)\delta(y_2) \left(2\ln\frac{\Delta}{Y} + \frac{3}{2} \right) \right] \Sigma_s\,. \tag{4.3}$$

In this case the parameter θ_0', that separated the kinematic regions *ii)* and *iii)*, only plays the role of an auxiliary one; it has already cancelled in the above expression for the cross section.

As we will see below, this situation is quite different for the experimentally more realistic, calorimetric set-up, when the detector cannot distinguish between events with a bare electron and events when the electron is accompanied by a hard photon emitted within a small cone with opening angle $2\theta_0'$ around the direction of the scattered electron. For this case we obtain

$$\Sigma_f = \Sigma_f^{cal} = P(z, L_0) \left[\frac{1}{2}\tilde{\Sigma} + \ln\frac{2(1-c)}{\theta_0'^2} \int\limits_0^{\infty} \frac{\mathrm{d}y_2}{y_2} \frac{1 + (1+y_2)^2}{1+y_2} \times \right.$$
$$\left. \times \left(\Sigma_s \Theta(y_2^{\max} - y_2) - \frac{\tilde{\Sigma}}{(1+y_2)^2} \right) \right]. \tag{4.4}$$

For the calorimetric event selection the parameter θ_0' is a physical one and the final result therefore does depend on it. However, the mass singularity that is connected

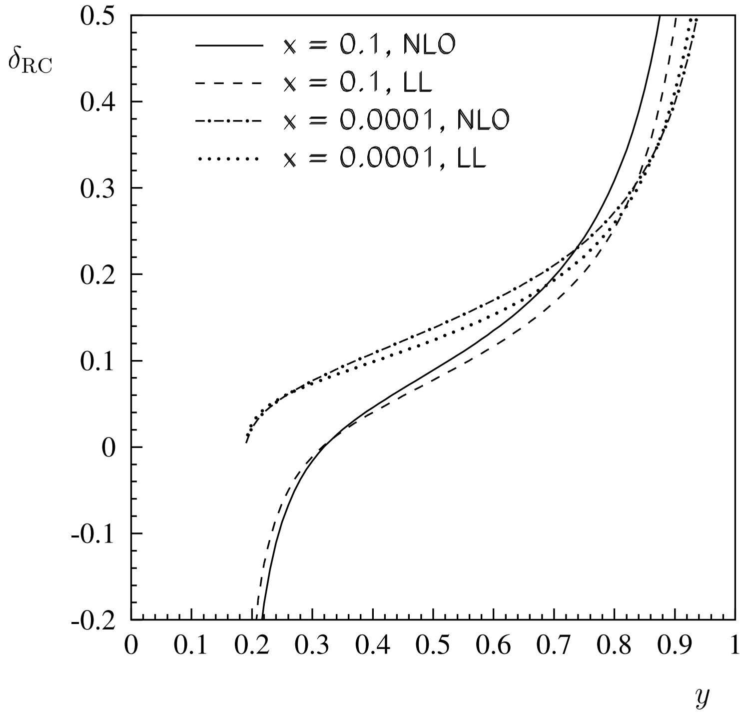

Figure 1: Radiative corrections $\delta_{\rm RC}$ (4.6) at leading and next-to-leading order for standard Bjorken variables for $x = 0.1$ and $x = 10^{-4}$ and a tagged photon energy of 5 GeV.

with the emission of the photon off the scattered electron is cancelled in accordance with the Kinoshita-Lee-Nauenberg theorem [17].

Note that the case of a coarse detector for the scattered electron, i.e., $\theta_0' \sim \mathcal{O}(1)$, agrees at the level of leading logarithms with the result of paper [11], that was obtained in the approximation of absence of emission along the scattered electron. Our result disagrees with the result of Bardin et al. [6] on the radiative corrections, as they neglected the interference of the emission of two photons; see [11] for a detailed discussion.

Finally we will give some numerical values obtained for the radiative corrections at leading and next-to-leading order for the experimentally relevant case of the calorimetric event selection with a realistic resolution. As input we used

$$E_e = 27.5 \text{ GeV}\,, \quad E_p = 820 \text{ GeV}\,, \quad \theta_0 = 0.5 \text{ mrad}\,, \tag{4.5}$$

whereas for the resolution of the detector we assumed $\theta_0' = 50$ mrad. As structure function we chose the ALLM97 parameterization [18] with $R = 0$. No cuts were applied to the photon phase space.

Figure 1 compares the radiative correction

$$\delta_{\rm RC} = \frac{{\rm d}^3\sigma}{{\rm d}^3\sigma_{\rm Born}} - 1 \tag{4.6}$$

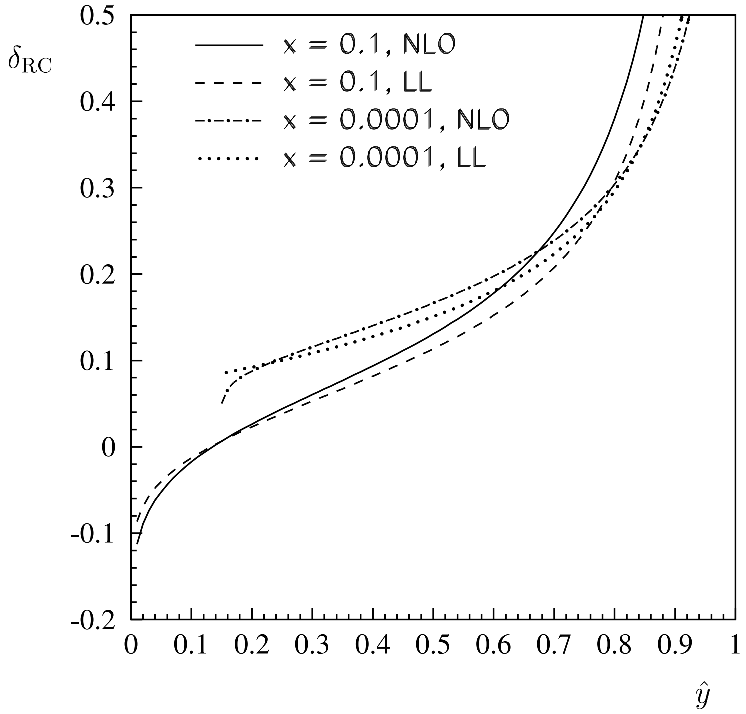

Figure 2: Radiative corrections $\delta_{\rm RC}$ (4.6) at leading and next-to-leading order for shifted Bjorken variables for $\hat{x} = 0.1$ and $\hat{x} = 10^{-4}$ and a tagged photon energy of 5 GeV.

at leading and next-to-leading order for the measurement in terms of the standard Bjorken variables x and y for $x = 0.1$ and $x = 10^{-4}$ for a tagged energy of $E_{\rm PD} = 5$ GeV. The typical size of the next-to-leading order contributions with respect to the leading-logarithmic result [11] amount to up to the order of 5%, depending on the kinematic region. The apparent cutoff in the curves at low y appears at

$$y_{\rm Bj,min} = \frac{1-z}{1-xz} \tag{4.7}$$

due to the condition that $\hat{x} \leq 1$, see eq. (1.5).

For the case of the shifted Bjorken variables (1.4) we present the corresponding result in fig. 2. Here no lower cut in $\hat{y}$ appears, like in the case of standard Bjorken variables. However, the curves for small $\hat{x} = 10^{-4}$ are not continued below the value of $\hat{y}$ where the cones with opening angles $2\theta_0$ (PD) and $2\theta_0'$ (calorimeter resolution) would start to overlap, as $\hat{y} \to 0$ corresponds to forward scattering. The difference of the radiative corrections between leading and next-to-leading order in this case also amounts to the order of 5%.

Lastly, in order to exhibit the z-dependence of the next-to-leading order contributions, i.e., the dependence on the energy in the photon tagger, we plot the corrections for $E_{\rm PD} = 20$ GeV in fig. 3 for $\hat{x} = 0.1$ and $\hat{x} = 10^{-4}$. One sees in particular the increasing

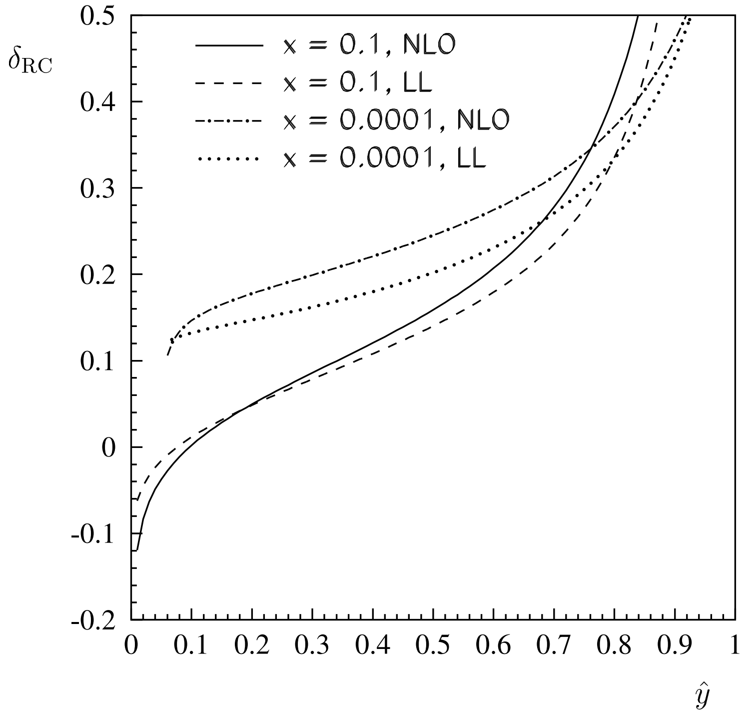

Figure 3: Radiative corrections δ_{RC} (4.6) at leading and next-to-leading order for shifted Bjorken variables for $\hat{x} = 0.1$ and $\hat{x} = 10^{-4}$ and a tagged photon energy of 20 GeV.

relevance of the next-to-leading order terms for large E_{PD} and in the experimentally interesting range of small $\hat{x}$.

We note in conclusion that the set of Feynman diagrams considered here is gauge invariant and model independent but not complete. We have neglected the contributions with two virtual photons exchanged between electron and the target that appear at the same order of perturbation theory, as well as the interference with the contributions when the second photon is emitted by the hadronic side. (These contributions have not yet been considered in any literature about DIS known to the authors). However, the description of this part is definitely model dependent and will be discussed elsewhere.

Acknowledgments

The authors are indebted to D. Bardin, E. Boos, L. Kalinovskaya, T. Ohl, T. Riemann, and L. Trentadue for useful discussions and interest in the problem considered. H.A. would like to thank L. Favart, M. Fleischer, and S. Schleif for continued interest. This work was supported in part by INTAS grant 93–1867 ext., and the Heisenberg-Landau program.

A. List of angular integrals for virtual corrections

In this section we collect the results of the angular integration of the definite structures of the Compton tensor in [13]. Using integrals similarly to (2.5) and retaining only terms that contain at least one large logarithm L_0 or L_Q, we obtain

$$
\begin{aligned}
\frac{2\varepsilon^2}{Q_l^2}\int\frac{\mathrm{d}\Omega_k}{2\pi}T_g &= -\rho\Big[\frac{1+z^2}{(1-z)^2}(L_0-1)+1\Big]+\frac{1+z^2}{(1-z)^2}[A\ln z+B]-\frac{4z}{(1-z)^2}L_Q\ln z-\\
&\quad-\frac{2-(1-z)^2}{2(1-z)^2}L_0\,,\\
2\varepsilon^2\int\frac{\mathrm{d}\Omega_k}{2\pi}T_{11} &= \frac{4z}{(1-z)^2}\rho L_0-\frac{2z(1+(1-z)^2)}{(1-z)^4}(A\ln z+B)-A\frac{z(3-z)}{(1-z)^3}+\\
&\quad+\frac{2L_0}{(1-z)^3}\Big(\frac{z(8z-3)}{1-z}\ln z+2z+z^2\Big)\,,\\
2\varepsilon^2\int\frac{\mathrm{d}\Omega_k}{2\pi}T_{22} &= \rho\Big(\frac{4z}{(1-z)^2}L_0-\frac{8}{(1-z)^2}\Big)+\frac{16}{(1-z)^2}\ln zL_Q-\\
&\quad-\frac{2z(1+2(1-z)^2)}{(1-z)^4}(A\ln z+B)-A\frac{3z-1}{z(1-z)^3}+\\
&\quad+\frac{2L_0}{z(1-z)^3}\Big(\frac{1+4z(z^2+z-1)}{1-z}\ln z+z^3-z^2+4z-1\Big)\,,\\
2\varepsilon^2\int\frac{\mathrm{d}\Omega_k}{2\pi}T_{21} &= \frac{2z^2}{(1-z)^4}(A\ln z+B)+\frac{3z-1}{(1-z)^3}A+\\
&\quad+\frac{2L_0}{(1-z)^3}\Big(\frac{-1+4z-4z^2-4z^3}{1-z}\ln z-2z^2-2z+1\Big)\,,\\
2\varepsilon^2\int\frac{\mathrm{d}\Omega_k}{2\pi}T_{12} &= \frac{2z(2-z)}{(1-z)^4}(A\ln z+B)+\frac{3-z}{(1-z)^3}A+\frac{2L_0}{(1-z)^3}\Big(\frac{3-8z}{1-z}\ln z-1-2z\Big)\,,
\end{aligned}
\tag{A.1}
$$

where ρ, A and B are given by eq. (2.6). It is remarkable to see that the relation

$$
\int\frac{\mathrm{d}\Omega_k}{2\pi}\Big[4zT_g+Q_l^2(T_{11}+z^2T_{22}+zT_{12}+zT_{21})\Big]=0 \tag{A.2}
$$

is fulfilled, leading to the factorization of the virtual corrections in eq. (2.6).

B. Angular integration for bremsstrahlung corrections

To perform the angular integration in (3.7) we first represent the integrand in the form

$$
\frac{\varepsilon^2\alpha^2(Q_{sc}^2)I^\gamma}{Q_{sc}^4}=\frac{F(t_1,t_2)}{t_1t_2}\,, \tag{B.1}
$$

where $t_{1,2}=(1-c_{1,2})/2$, $c_{1,2}=\cos\theta_{1,2}$, and $\theta_{1,2}$ are the angles between non-tagged photon momentum k_2 and the momenta of the initial and the scattered electrons. Note that $F(t_1,t_2)$ behaves regularly for $t_1\to 0$ or $t_2\to 0$. This can be easily seen by considering the limiting cases for the quantity I^γ.

For the case $t \to 0$, which corresponds to the the second photon being emitted close to the direction of the incoming electron, one obtains from eq. (3.8)

$$
\begin{aligned}
I^\gamma|_{t\to 0} = & \frac{Q^2}{x_2 t}(z^2 + (z-x_2)^2) \times \\
& \times \left[x_t F_2(x_t, Q_t^2) \left(\frac{M^2}{Q_t^2} - \frac{1-y}{x^2 y^2 (z-x_2)} \right) - F_1(x_t, Q_t^2) \right], \qquad \text{(B.2)}
\end{aligned}
$$

while for the case $s \to 0$, corresponding to the second photon being almost collinear to the final electron,

$$
\begin{aligned}
I^\gamma|_{s\to 0} = & -\frac{Q^2 z}{y_2 s}(1 + (1+y_2)^2) \times \\
& \times \left[x_b F_2(x_b, Q_b^2) \left(\frac{M^2}{Q_b^2} - \frac{1-y}{x^2 y^2 z (1+y_2)} \right) - F_1(x_b, Q_b^2) \right], \qquad \text{(B.3)}
\end{aligned}
$$

see eqs.(3.4) and (3.12) for the notation. The r.h.s. of eq. (B.1) is easily seen to be

$$
\left. \frac{\varepsilon^2 \alpha^2 (Q_{sc}^2) I^\gamma}{Q_{sc}^4} \right|_{t\to 0} = \frac{1}{t_1 t_2} \frac{a}{16\pi x_2^2} \frac{z^2 + (z-x_2)^2}{z(z-x_2)} \Sigma(x_t, y_t, Q_t^2), \qquad \text{(B.4)}
$$

$$
\left. \frac{\varepsilon^2 \alpha^2 (Q_{sc}^2) I^\gamma}{Q_{sc}^4} \right|_{s\to 0} = \frac{1}{t_1 t_2} \frac{a}{16\pi x_2^2} \frac{1 + (1+y_2)^2}{1+y_2} \Sigma(x_b, y_b, Q_b^2), \qquad \text{(B.5)}
$$

where $a = (1 - \cos\theta)/2$.

For the phase space of the photon we use the following representation:

$$
\int \frac{\mathrm{d}^3 k_2}{\omega_2} = \varepsilon^2 \int x_2 \, \mathrm{d}x_2 \, \mathrm{d}\Omega_2 = 4\varepsilon^2 \int x_2 \, \mathrm{d}x_2 \int \frac{\mathrm{d}t_1 \, \mathrm{d}t_2}{\sqrt{D}} \Theta(D), \qquad \text{(B.6)}
$$

$$
D = (t_2 - y_-)(y_+ - t_2), \quad y_\pm = t_1(1-2a) + a \pm 2\sqrt{a(1-a)t_1(1-t_1)}.
$$

The region of integration is determined by the conditions

$$
\sigma_1 < t_1 < 1, \quad \sigma_2 < t_2 < 1, \quad D > 0, \quad \sigma_1 = \frac{\theta_0^2}{4}, \quad \sigma_2 = \frac{\theta_0'^2}{4}. \qquad \text{(B.7)}
$$

Using the substitution

$$
t_2 \to t_2(t_1, u) = \frac{(a-t_1)^2(1+u^2)}{y_+ + u^2 y_-}, \qquad \text{(B.8)}
$$

and the identity

$$
\begin{aligned}
\int_{\sigma_1}^{1} \mathrm{d}t_1 \int_{\sigma_2}^{1} \mathrm{d}t_2 \frac{F(t_1,t_2)}{t_1 t_2 \sqrt{D}} \Theta(D) = & \frac{\pi}{a} \left[F(a,0) \ln \frac{a}{\sigma_2} + F(0,a) \ln \frac{a}{\sigma_1} \right] + \\
& + 2 \int_0^\infty \frac{\mathrm{d}u}{1+u^2} \lim_{\eta\to 0} \left[\int_\eta^1 \frac{\mathrm{d}t_1}{t_1 |t_1 - a|} (F(t_1,t_2) - F(a,0)) + \right. \\
& \left. + \int_\eta^a \frac{\mathrm{d}t_1}{t_1 a} (F(a,0) - F(0,a)) \right], \qquad \text{(B.9)}
\end{aligned}
$$

which is valid for $\sigma_1, \sigma_2 \ll a$, we obtain for Z from eq. (3.9) the following expression:

$$Z = -\frac{4(1-c)}{zQ^2}\int\limits_0^\infty \frac{\mathrm{d}u}{1+u^2}\Bigg[\int\limits_\eta^1 \frac{\mathrm{d}t_1}{t_1|t_1-a|}\int\limits_0^{x_m}\frac{\mathrm{d}x_2}{x_2}(\Phi(t_1,t_2(t_1,u))-\Phi(a,0)) + \\ + \int\limits_\eta^a \frac{\mathrm{d}t_1}{t_1 a}\int\limits_0^{x_m}\frac{\mathrm{d}x_2}{x_2}(\Phi(a,0)-\Phi(0,a))\Bigg]_{\eta\to 0}, \tag{B.10}$$

where

$$\Phi(t_1,t_2) = \frac{\alpha^2(Q^2_{sc})stI^\gamma}{Q^4_{sc}}\Bigg|_{c_1=1-2t_1,\ c_2=1-2t_2(t_1,u),\ c=1-2a}. \tag{B.11}$$

The upper limit of the x_2-integration, x_m, may be deduced from [6]. It has the form

$$x_m = \frac{z(e+p)-\Delta_m - Y(e+z)-(p-z)Yc}{z+e-Y+(p-z)c_1+Yc_2}, \qquad e = \frac{E_p}{\varepsilon}, \\ p = \frac{P_p}{\varepsilon}, \qquad \Delta_m = \frac{(M+m_\pi)^2-M^2}{2\varepsilon^2}. \tag{B.12}$$

This finally leads to eq. (3.9).

It is important to note that when calculating Z one encounters neither collinear nor infrared singularities.

References

[1] L. Mo and Y. Tsai, *Rev. Mod. Phys.* **41** (1969) 205.

[2] H. Spiesberger (convener), et al., *Radiative Corrections at HERA*, in *Physics at HERA*, edited by W. Buchmüller and G. Ingelman, DESY, Hamburg, 1991.

[3] A. Akhundov, D. Bardin, L. Kalinovskaya and T. Riemann, *Fortsch. Phys.* **44** (1996) 373.

[4] S. Jadach, M. Jezabek and W. Płaczek, *Phys. Lett.* **B 248** (1990) 417.

[5] M.W. Krasny, W. Płaczek and H. Spiesberger, *Z. Physik* **C 53** (1992) 687.

[6] D. Bardin, L. Kalinovskaya, T. Riemann, *Z. Physik* **C 76** (1997) 487 [hep-ph/9612203].

[7] T. Ahmed et al., H1 Collaboration, *Z. Physik* **C 66** (1995) 529.

[8] L. Favart, M. Gruwé, P. Marage and Z. Zhang, *Z. Physik* **C 72** (1996) 425 [hep-ph/9606465].

[9] H1 collaboration: talk no. 404 given by M. Klein at the *ICHEP98 conference, Vancouver, Canada, July 1998*, and contributed paper no. 535.

[10] A.B. Arbuzov et al., *Nucl. Phys.* **B 485** (1997) 457 [hep-ph/9512344]; N.P. Merenkov et al., *Acta Phys. Pol.* **B 28** (1997) 491; *Phys. Lett.* **B 394** (1997) 218 [hep-ph/9606425].

[11] H. Anlauf, A.B. Arbuzov, E.A. Kuraev, N.P. Merenkov, to appear in *Phys. Rev.* **D** [hep-ph/9711333].

[12] H. Anlauf, A.B. Arbuzov, E.A. Kuraev, N.P. Merenkov, *JETP Lett.* **66** (1997) 391; Erratum, *ibid.* **67** (1998) 305.

[13] E.A. Kuraev, N.P. Merenkov, V.S. Fadin, *Sov. J. Nucl. Phys.* **45** (1987) 486.

[14] R.P. Feynman, *Photon-Hadron Interactions,* W.A. Benjamin, Inc., Reading, Massachusetts, 1972.

[15] V.N. Baier, V.S. Fadin and V.A. Khoze, *Nucl. Phys.* **B 65** (1973) 381.

[16] N.P. Merenkov, *Sov. J. Nucl. Phys.* **48** (1988) 1073.

[17] T. Kinoshita, *J. Math. Phys.* **3** (1962) 650; T.D. Lee and M. Nauenberg, *Phys. Rev.* **133** (1964) 1549.

[18] H. Abramowicz, A. Levy, Preprint DESY-97-251, hep-ph/9712415.